ELSEVIER

Surface and Coatings Technology 140 (2001) 82–92

SURFACE & COATINGS TECHNOLOGY

www.elsevier.nl/locate/surfcoat

Characterization of large area filtered arc deposition technology: part I — plasma processing parameters

Vladimir I. Gorokhovsky[a,*], Rabi Bhattacharya[b], Deepak G. Bhat[c]

[a]Arcomac Plasma Processing Lab, Toronto, Ontario, Canada
[b]UES Incorporated, Dayton, OH, USA
[c]Stellram Incorporated, La Vergne, TN, USA

Received 14 April 2000; accepted in revised form 20 January 2001

Abstract

The transmission of metal–gas plasma flow generated by large area, rectangular dual-filtered-arc source is investigated. The characteristic parameters of plasma flow such as ion current yield and inter-electrode voltage drop vs. gas pressure, are established for the deposition of TiN coatings. The uniformity and productivity of coating deposition on complex parts in a 3D operational volume is determined. It is found that ion current yield increases from 6 to 10 A with increasing argon pressure in the range of $2–7\times10^{-2}$ Pa. It results in a deposition rate on the order 1–2 μm/h in a double rotation mode. It is shown that a thickness uniformity of $\pm10\%$ or better can be achieved in a programmable, vertical scanning mode. © 2001 Elsevier Science B.V. All rights reserved.

Keywords: Vacuum arc; Filtered arc; Uniformity; Ion current; Multilayer; Plasma immersion

1. Introduction

Vacuum arc discharge plasma has been used successfully in the last two decades for the deposition of hard coatings for cutting tools and machine parts. In this process, a jet of highly ionized metal plasma, flowing from the cathodic arc spot, transfers coating material from the target to the substrate surface. A significant disadvantage of this method is the formation of droplets (also known as macro-particles) in the cathodic arc jets, which limit the application of the process to surface coatings that do not require high precision or surface finish. These particles also deleteriously influence critical properties of the coatings [1]. For instance, in the case of TiN coating on cutting tools, the presence of titanium particles in the coating compromises the hardness and wear resistance of the coating itself.

The filtered arc source allows deposition of droplet-free coatings by deflecting the plasma flow along the curvilinear magnetic lines of force towards the substrate, while the droplets, having straight trajectories, are captured on the baffles. Thus, a fully ionized flow of metal plasma is directed to the substrate. One of the first macroparticle filter designs was based on the plasma–optical principle [2]. It was a quarter-torus tubular electromagnetic plasma guide, and was based on the torus-type plasma traps, which were previously well-known in controlled nuclear fusion apparatus such as the Stellarator and Tokamak. However, in contrast to the plasma fusion apparatus, the vacuum arc plasma guide utilizes relatively low magnetic fields (typically 5–20 mT in the center of the plasma duct). This field magnetizes the electron component of arc plasma jet, whilst the trajectory of ions is governed by the trans-

* Corresponding author. Tel.: +1-416-534-1073; fax: +1-416-534-4502.
E-mail address: arcomac@sympatico.ca (V.I. Gorokhovsky).

PII: S0257-8972(01)01022-2

verse electrostatic field created in a polarized plasma column. This type of filter removed the macro-particles and achieved deposition rates for titanium metal films up to 40 μm/h on a substrate installed in front of the filter exit. However, it could operate only with small cylindrical cathode targets, and could not be scaled up due to the difficulty of scaling up the filter apparatus using cylindrical magnetic coils.

The tubular, cathodic-arc macro-particle filters available in the market today are based on this original work, and suffer from the same limitations. Up to now, the commercially available, filtered arc sources can only provide a limited deposition area. Detailed reviews of the various filtering techniques and apparatus were published recently [3,4]. These reviews have highlighted the basic concepts used in various modifications of the original filter design of Aksenov et al. [2]. For instance, the CAF-38 source from the Commonwealth Scientific Corporation, consists of a tubular plasma duct of 10 cm internal diameter, which provides a plasma beam diameter of approximately 50 mm. Using magnetic rastering, this source can cover a maximum width of approximately 150-mm coating area with acceptable uniformity only near the center of the deposition spot [5]. Filtered arc sources produced by CSIRO in Australia are based on the original design of FAD sources used in Russia in the 1970s, and provide a 100-mm diameter coating area. Aksenov et al. in a recent publication [6] presented the results of testing a tubular rectilinear filtered arc source with improved productivity. The ion current yield at the exit of this source with Ti target ranges from 1.4 to 1.7 A for a 130-A cathode current. The uniformity of the coating distribution at the exit plane of this source is limited by the diameter of the source (approx. 300 mm), which is typical for tubular type, cathodic arc sources.

Another disadvantage of the existing state-of-the-art filtered-arc source technology is the relatively low level of ionization of reaction gas, such as nitrogen or oxygen. In comparison with the nearly 100% ionization of metal plasma, the average ionization rate of gaseous plasma component can be less than 1% [1,3]. Martin et al. [7] recently showed that a significant improvement of coating properties can be achieved by gaseous ion-assisted filtered arc deposition (FAD), in which the ratio of metal to gaseous ions can be controlled. In this work, an independent gaseous ion source was used to provide a gaseous ion beam along with a metal plasma stream of the filtered arc source.

The foregoing limitations of tubular filter design have been recognized for some time, leading to attempts at developing linear, rectangular filtered-arc sources. One such approach by Welty [8,9] aims at deposition on large areas in a practically scalable design. This design consists of a rectangular vacuum arc plasma source and associated apparatus in which a rectangular planar cathode is mounted in a rectangular plasma duct. Magnets control the arc motion on the cathode surface while simultaneously generating the magnetic field, which guides the plasma through the duct. When the arc spot has moved to one end of the rectangular target, the magnetic field is reversed so that the arc moves back to the other end of the target. The motion of the arc spot is thus controlled by a rapidly reversing magnetic field. In the other embodiment of this design, the filter assembly is placed in the center of the deposition chamber, such that the rectangular target is shielded on both sides by extended baffles to prevent the macroparticles from being transported to the substrate. The flux of ionized metal is thus bent around the extended baffles for a relatively droplet-free coating.

Limited scale-up potential of conventional, filtered arc systems appears to be a serious obstacle for industrial applications of cathodic arc deposition technology. This paper represents the results of assessment of novel large area, filtered arc surface engineering technology, integrated in an industrial vacuum chamber layout.

2. Characterization of plasma processing in large area, filtered arc plasma immersion surface engineering systems

The rectangular large area filtered arc source (LAFAS) now commercially available from Arcomac Plasma Processing Lab, overcomes the limitations of the previous filter designs [10]. Fig. 1 shows a schematic view of the large area, filtered-arc deposition (LAFAD) universal surface engineering system layout incorporating two LAFAS sources. The LAFAS uses a rectangular plasma-guide chamber with two rectangular deflecting coils installed on the opposite sides. In this design, two or more cylindrical or two rectangular primary cathodic arc sources are placed opposite each other on the side walls of the plasma-guide chamber, surrounded by rectangular deflecting coils, and separated by an anodic baffle plate. The source uses a superimposed deflecting magnetic field to turn the metal ion flow 90° towards the deposition chamber. A set of scanning magnetic coils allows the ion plasma jet to be swept in the vertical direction so as to cover significantly large surface areas. At the same time, the arc column is well confined by a magnetic field in the horizontal direction, providing enhanced suppression of the turbulent plasma diffusion and leading to a significant increase in the metal vapor ion yield [10,11].

The LAFAS plasma source used in this work utilized two primary direct cathodic arc evaporators attached to opposite walls of the rectangular LAFAS plasma guide chamber — 350 mm wide × 450 mm high × 500 mm

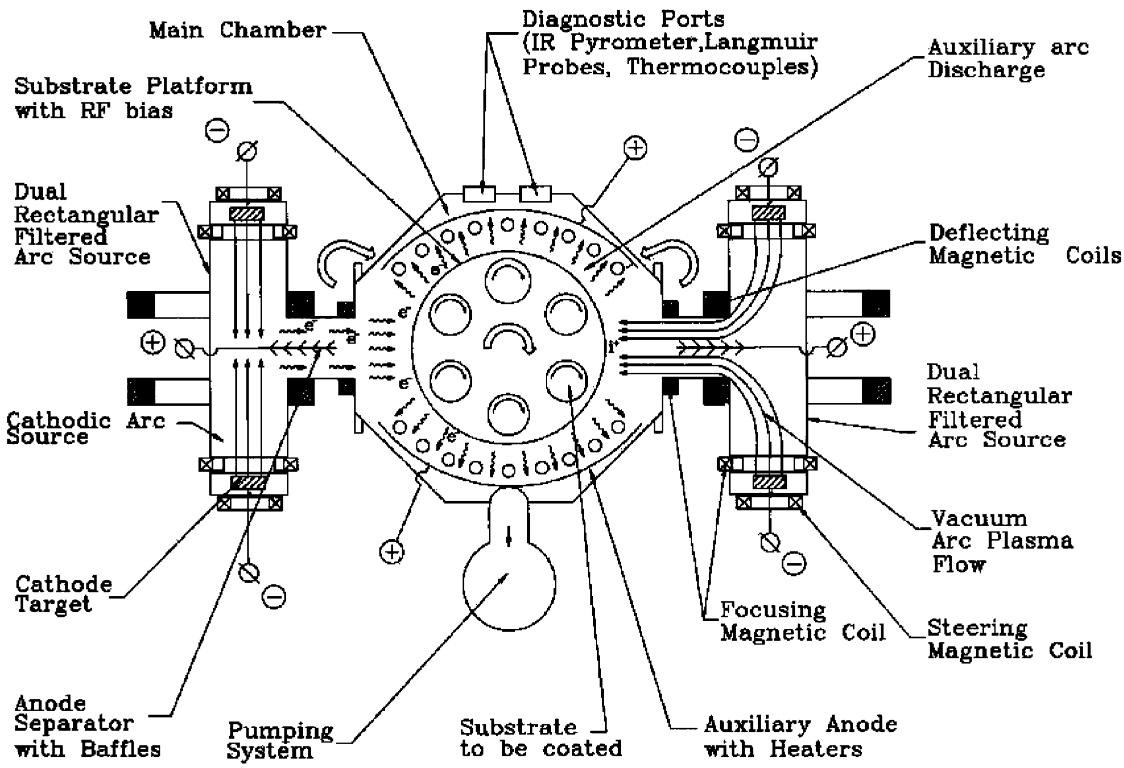

Fig. 1. Large area, dual-filtered arc surface engineering system layout.

deep. These evaporators consisted of impulse high voltage igniters, magnetic steering and focusing coils, and round titanium targets (80 mm diam. × 50 mm height). The anode separator installed along the plane of symmetry of the plasma-guide chamber used a water-cooled St.St. plate (12 mm thick × 400 mm wide × 300 mm high), with a set of vertical stainless steel baffles (2 mm thick × 12 mm wide × 300 mm high), attached to both sides of the anode separator plate at a distance of 12 mm between each other. The deflecting magnetic field was set to 5 mT in the center of the plasma guide chamber for all experiments described in this paper. The total ion saturation current yield of the LAFAS plasma source was measured by a flat collector plate, which fully overlapped the exit flange of the LAFAS, having an opening (300 mm wide × 400 mm high) towards the main chamber. The collector was set at a bias voltage of -100 V with respect to the ground during ion current measurements. Argon was used as a gaseous environment for measuring characteristic plasma parameters of the LAFAS.

Fig. 2a, curve 1, shows the total ion current yield vs. gas pressure at the exit of the dual arc LAFAS plasma source. The total ion current yield increases from 6 to 10 A when the argon pressure was increased from 2 to 7×10^{-2} Pa, indicating the contribution of the gaseous plasma component in the total ion current yield of the LAFAS plasma source. The ion current yield does not decrease when the argon pressure is less than 10^{-2} Pa, which permits an estimate of the contribution of the metal plasma current of approximately 5–6 A; whilst each of the primary cathodic arc sources of LAFAS plasma operate at 100–120 A. At the same time, it shows that the gaseous plasma can contribute approximately 30–40% of the total ion current yield of LAFAS plasma source in the pressure range 10^{-2}–10^{-1} Pa. The high yield of ionized gases provided by the LAFAS plasma source is due to the large volume of the plasma guide chamber where the electron density is maximum, as it is determined by the balance between the volumetric ionization by electron impact and the decay channel — plasma losses on the walls of the unit. The ion current of the LAFAS also increases with the current of the primary cathodic arc sources, indicating the relationship between the ion current yield at the exit plane of the filtered arc source and the amount of metal plasma generated by the primary cathodic arc sources of the LAFAS plasma source.

The influence of the anode separator on the total ion current yield of the LAFAS is shown in Fig. 2b, curves 5–7. The increase in the ion current yield of the LAFAS with increasing anode separator current is due to an increase in the voltage drop between the anode separator and the surrounding wall of the plasma guide chamber (Fig. 2b, curves 1–4). This repels the arc plasma ions toward the coating chamber. The effectiveness of the ion current transfer capability of the LAFAS can be estimated to be up to 3–5 times higher

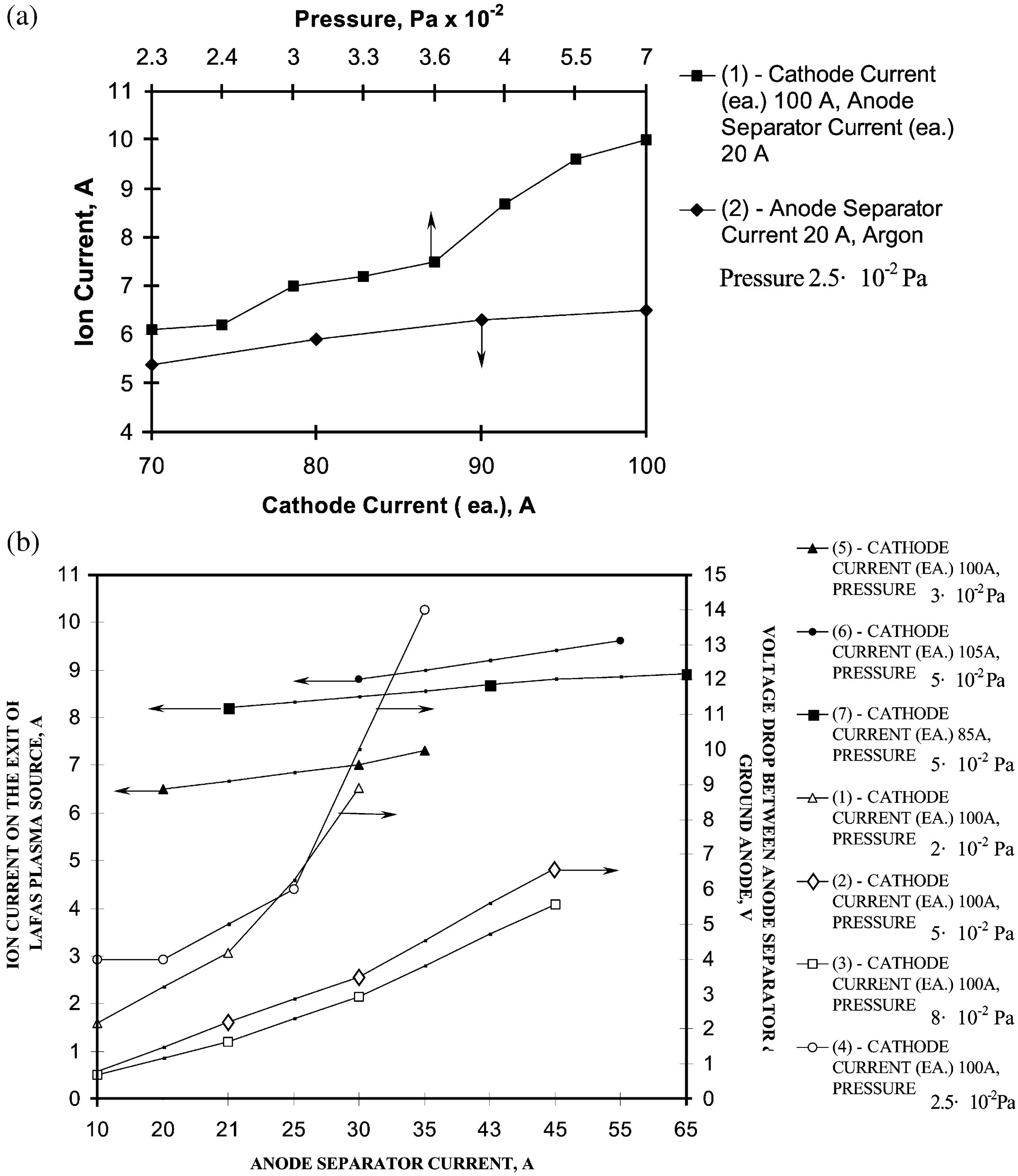

Fig. 2. Characteristic parameters of a LAFAS-500C plasma source with titanium targets in argon vs. argon pressure: (a) LAFAS ion current yield vs. argon pressure (1) and arc current of each target (2); (b) voltage–current characteristics of anode separator (1–4) and ion current yield vs. anode separator current (5–7).

than the conventional single channel, tubular FAD source [1,6]; whilst the absolute value of the total ion current at the exit of a dual arc LAFAS plasma source exceeds the typical ion current produced by the conventional vacuum arc evaporator, typically ranging from 4 to 8 A [1]. This advanced filter design provides a practically droplet-free coating on large areas, ranging from approximately 250 mm in width to heights in the order of 300 mm to 2 m or more. In the filtered arc coating deposition mode, the deflecting magnetic field is turned on at least in one of the LAFAS sources. The LAFAS plasma contains a fully-ionized flow of target cathode vapor, and a relatively highly dissociated, ionized and activated reactive gas. This leads to a maximum flux of bombarding ions on the substrate surface. As a result, it is possible to produce dense and adherent coatings with highly disordered structures and unique properties. Examples of coatings deposited using the large area, filtered arc sources are given in part II of this paper.

The vacuum arc cathode is also a theoretically unlimited electron emitter, thus providing an efficient source of high-density electron current [11,13,14]. When the deflecting magnetic field of the LAFAS plasma source is not activated in the auxiliary-arc plasma immersion mode, it facilitates the generation of a uniform, high-density plasma cloud in the process chamber. This results in a 'plasma immersion' environment [12,14], which provides a uniform condition for plasma ion etching, ion nitriding, low energy ion implantation and plasma-assisted chemical vapor deposition.

The auxiliary arc plasma immersion mode is supported by a set of auxiliary anodes, installed in the main chamber of the LAFAD system, and provides an auxiliary arc discharge, which fills the entire operating space of the chamber with a highly-ionized and dense plasma environment, as schematically shown in Fig. 1, [12,14,15]. When the magnetic deflecting system of the LAFAS plasma source is turned off, the auxiliary arc discharge is established between the primary cathodes of LAFAS and the distant auxiliary anodes installed in the coating chamber (Fig. 1). Typically, the current of auxiliary arc discharge ranges from 30 to 100 A, while the cathode current of each primary cathodic arc source does not exceed 120 A. The ion-current density in the auxiliary arc discharge ranges from 0.1 to 10 mA/cm^2 in a pressure range of 10^{-3}–1 Pa. A typical relationship between gaseous plasma, ion saturation current and the auxiliary arc discharge current for different pressures is shown in Fig. 3 [11,12]. The ion saturation current in the auxiliary arc plasma decreases when argon pressure increases. Conversely, the rate of dissociation in the gaseous plasma environment increases when the pressure increases in the auxiliary arc discharge, due to dissociative recombination of molecular ions and direct dissociation of molecules by electron impact with the decay channel — heterogeneous recombination of atoms [11,12]. This is illustrated in Fig. 3, which shows the increase in the ion nitriding rate of high speed steel in a nitrogen auxiliary arc discharge plasma to the level of 40 μm/h, when the auxiliary anode current is increased to 200 A. In this experiment, the substrate temperature did not exceed 400°C which demonstrates the effectiveness of ion nitriding in auxiliary arc discharge at relatively low temperatures of steel substrates.

3. Uniformity and productivity of the LAFAD process

In a rectangular filter design, a high uniformity of coating thickness can be achieved by utilizing the rectangular cathode targets. The design of a rectangular cathodic arc source (compatible a with LAFAS plasma source) was shown in [16]. In this case, the equalization of erosion and transfer of target materials is achieved by a continuous movement of the cathodic arc spots around the operating area of the target. Some non-uniformity will occur only on the top and bottom portion of the coating zone due to the shadow effect of the top and bottom walls of plasma guide chamber, respectively. In the case of round targets, a superimposed vertical scanning magnetic field has to be applied to equalize the mean vertical distribution of erosion plasma flow transferring from the target surface towards the substrate to be coated.

In the present work, the coating chamber (600-mm diameter × 600 mm in height) was equipped with one LAFAS-600C source, containing two 80-mm (3 inch) diameter × 50-mm (2 inch) height titanium targets (Fig. 4). The LAFAS plasma source was attached to the door of the main chamber supported by a wheel-jack. The uniformity and productivity of the LAFAD process was characterized by processing sample coupons of two different types. The first set consisted of stainless steel bars of dimensions 25 × 12.5 × 356 mm (1 × 0.5 × 14

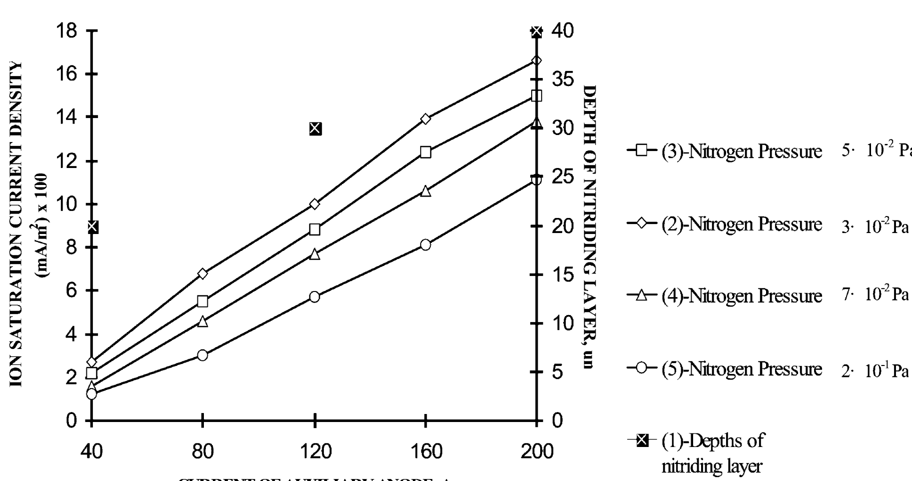

Fig. 3. Ion saturation current in auxiliary arc discharge vs. auxiliary anode current and rate of ion nitriding of HSS in auxiliary arc plasma (bias voltage −400 V, substrate temperature 400°C).

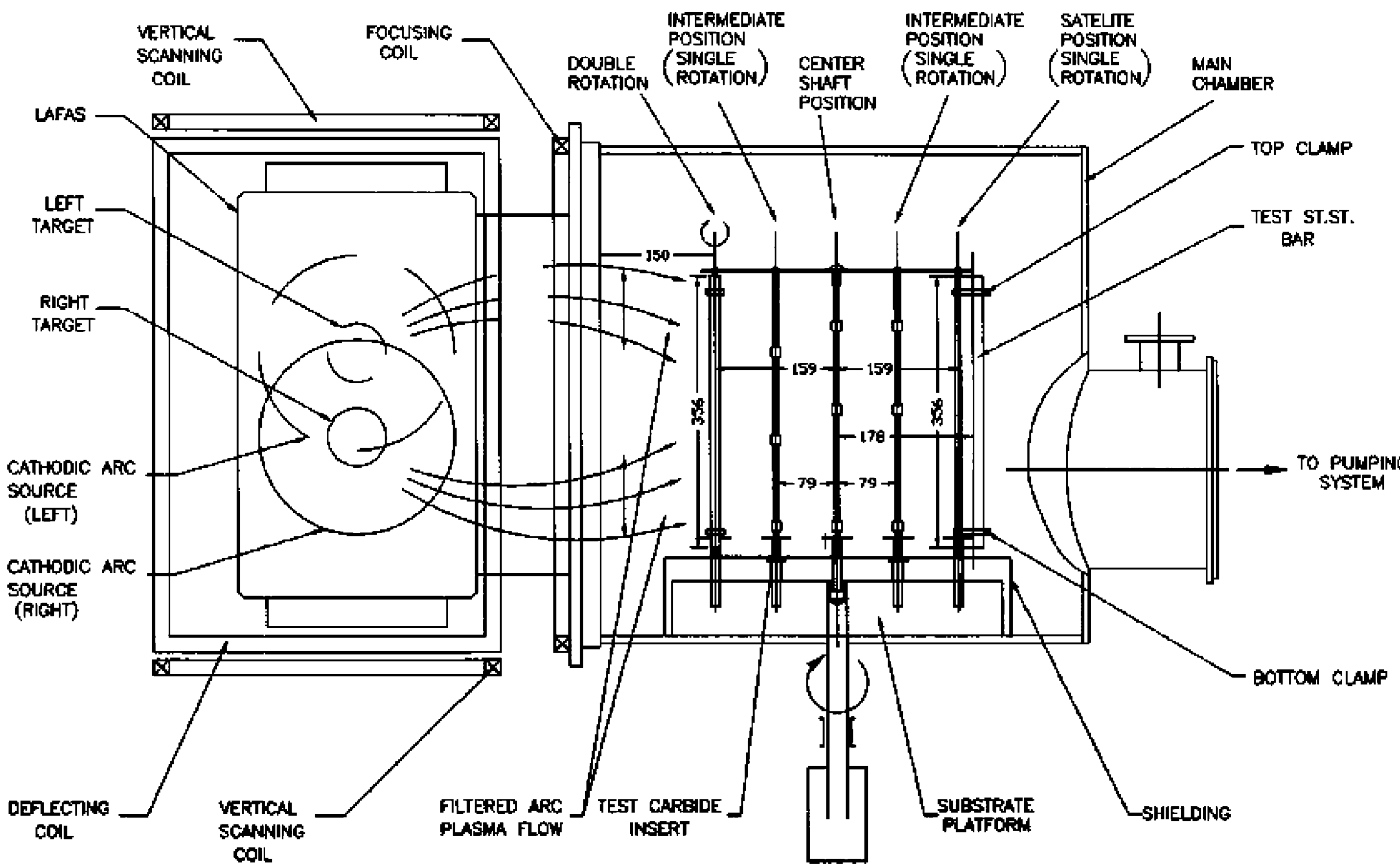

Fig. 4. System layout and fixture geometry for uniformity and productivity tests.

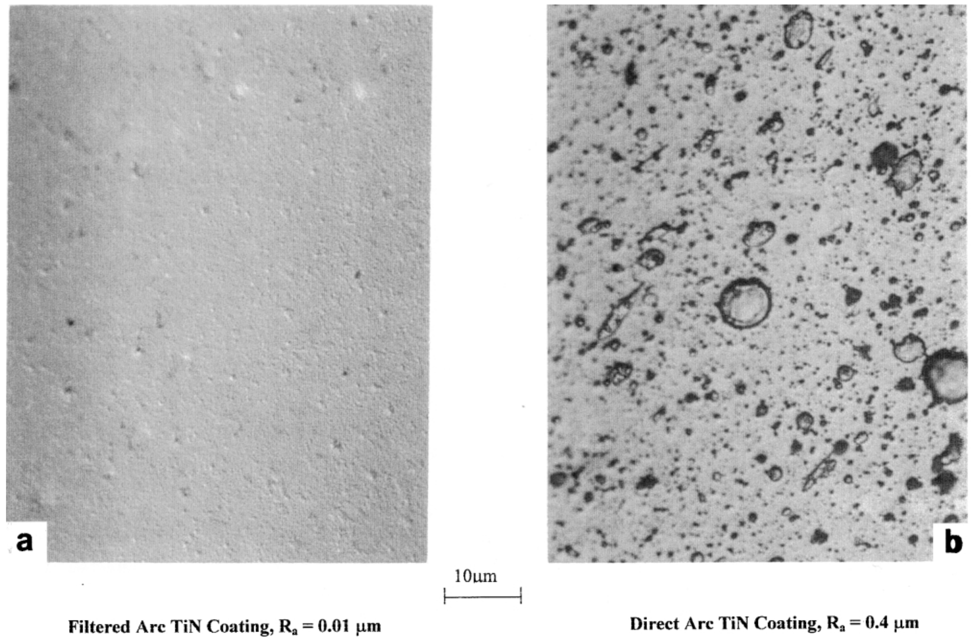

Fig. 5. Substrate surfaces with (a) filtered and (b) direct arc coatings — deposition time, 2 h.

inches) with a polished ($R_a < 100$ nm) front surface area of 25 × 356 mm (1 × 14 inches). The bars were clamped vertically at the top and bottom to the shaft-holders of satellites installed at three different distances from the center of the substrate platform, as shown in Fig. 4. The other set of samples was made of cemented carbide WC-6%Co inserts, 12 × 12 × 3.2 mm (0.5 × 0.5 × 0.125 inch) with a mirror-like finish on the front surface ($R_a < 20$ nm). The satellites installed at the center of the substrate platform and at the intermediate position had a single rotation whilst the satellites installed at the periphery of the substrate platform could be rotated in both single and double-rotation modes. For investigating coating thickness uniformity, all testing runs were carried out for 2 h for the deposition of a multilayer Ti/TiN coating. The time of Ti layer deposition was 5 min while each of the TiN layers was deposited for 25 min. The Ti coating was deposited in an argon atmosphere and the TiN layer was deposited in nitrogen. The process pressure was $2–3 \times 10^{-2}$ Pa during the deposition of both layers. The arc current for each titanium cathode ranged from 100 to 120 A. The coating thickness was measured by the CALOTEST ball wear-scar method.

Fig. 5 shows the surface of TiN coating with a 2-μm thickness, deposited on the carbide test insert by the LAFAS source in comparison with TiN coating deposited by conventional vacuum arc technique without electromagnetic filtering. It can been seen, that macroparticles are incorporated in the ion matrix deposit, creating a pattern of macro defects and porosity in the coating morphology. These α-Ti particles have no significant bonds both with the substrates and with the surrounding ion plasma matrix deposit, resulting in a significant reduction of adhesion and cohesion of coatings [1].

Fig. 6 shows the profilometry of the surface of highly polished M50 steel coupons (initial roughness less than 30 nm) with TiN coating deposited by the LAFAS filtered arc and conventional direct arc sources. The vacuum arc sources (identical to the primary cathodic arc sources of the LAFAS plasma source) were used for direct arc coating deposition process. The arc current of the primary cathodic arc sources of LAFAS was set at 100–120 A, while the arc current of direct cathodic arc sources was set to 60 A due to the necessity to reduce the macroparticle phase in direct arc coatings. Both coatings had a thickness of approximately 3 μm. The filtered arc coating shows a dramatic decrease in surface roughness.

The results of thickness measurements on steel bars with single and double rotation, installed at three different distances from the center of the substrate platform are given in Fig. 7. The deposition rate ranged from 0.9 to 1.4 μm/h for bars coated with double-rotation, while it reached 1.9 μm/h for substrates with single rotation.

In the direct-arc mode, the deposition is strictly line-of-sight, with some dispersion of the plasma jet. Consequently, the variation of coating thickness in the axial direction of the plasma jet is significant, and therefore most of the deposition occurs when the substrate is directly in front of the target. When double-rotation is added to the substrate, the deposition rate in a direct-arc deposition decreases by a factor of 3 or more. Thus, the thickness uniformity that can be

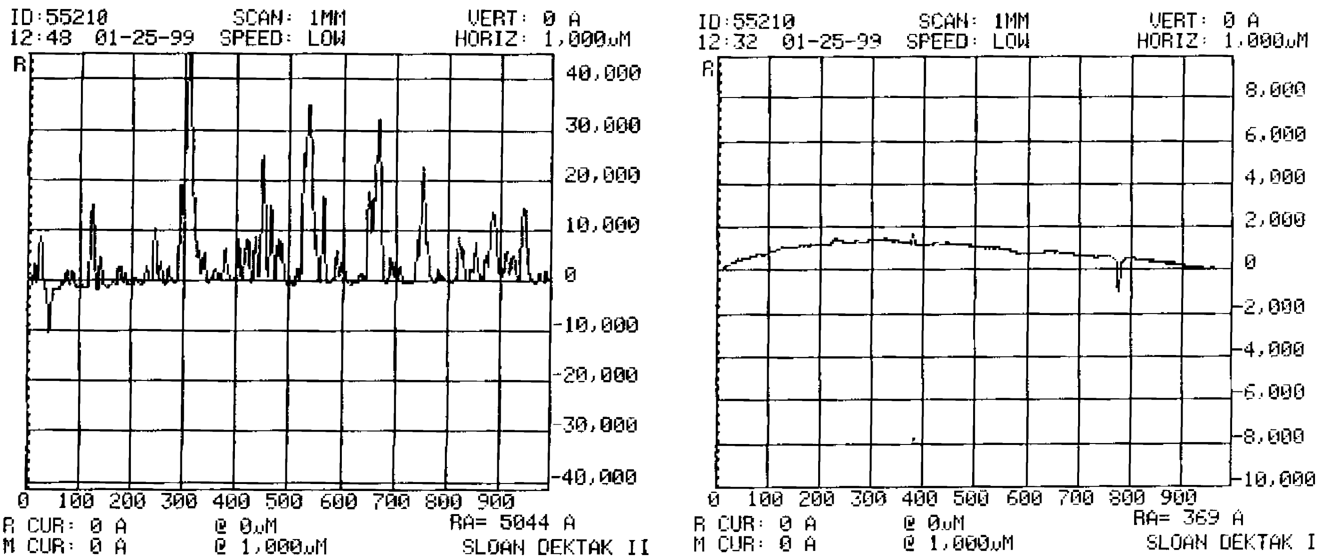

(a) **Direct Arc TiN Coating, R_a = 504 nm** (b) **Filtered Arc TiN Coating, R_a = 37 nm**

Fig. 6. Profilograms of highly polished M50 steel coupons with TiN coatings: (a) direct arc deposition, 3-μm coating thickness; and (b) LAFAD process, 2.8-μm coating thickness.

achieved in a direct-arc mode is severely limited in the 3-D space of the deposition chamber.

In the filtered-arc mode, it was found that the decrease in the deposition rate between single and double-rotation was only approximately half of that experienced in a direct arc mode (approx. 1.5–1.7:1). The ability to scan the plasma jet in the vertical direction, combined with the confinement of the plasma in the horizontal direction by the superimposed electromagnetic field, allows greater depth of penetration of the ionized flux in the axial direction of the plasma jet. This permits improved thickness uniformity on substrates placed across the full diameter of the platform. This aspect is described in the following paragraphs.

The uniformity of coating distribution can be controlled by the superimposed vertical scanning magnetic field. Fig. 8 shows the distribution of TiN coating thickness measured on carbide test inserts, placed along the axis of the substrate holder fixtures, which were installed at various distances from the center of substrate platform table, and subjected to single and double rotation. The results clearly demonstrate that a superimposed vertical scanning magnetic field can shift the coating distribution in the vertical direction. The proper cycle parameters, i.e. time of activation of the upward field ($t_{\uparrow}$) and time of activation of the downward field ($t_{\downarrow}$), can be found by iteration. In a programmable, vertical scanning mode it is possible to

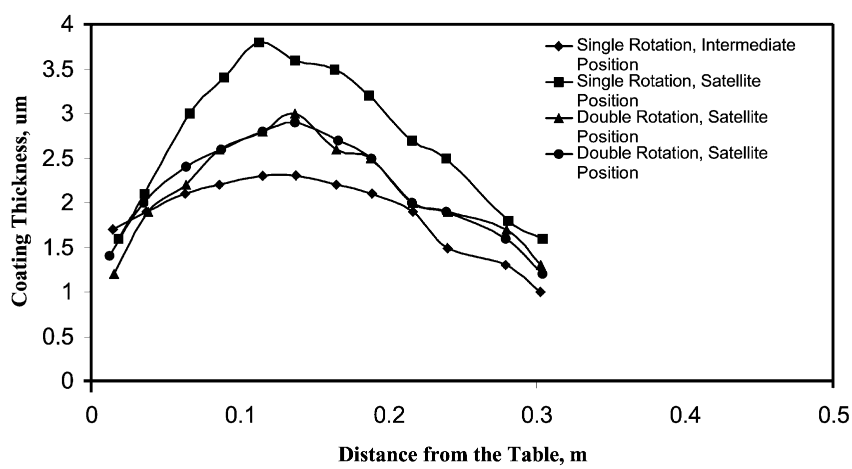

Fig. 7. Titanium nitride LAFAD coating thickness distribution along stainless steel bars with single and double rotation, installed on different distances from the center of the substrate platform — deposition time, 2 h.

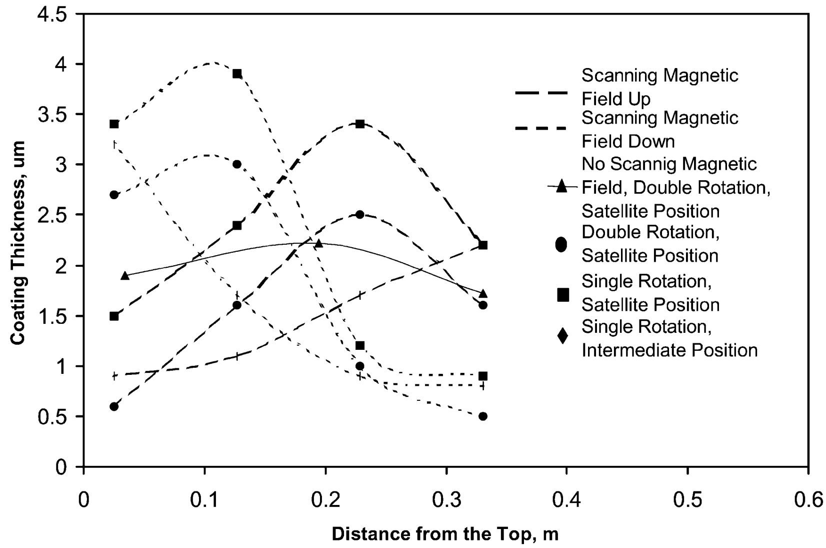

Fig. 8. Influence of the vertical scanning magnetic field on titanium nitride LAFAD coating thickness distribution on carbide coupons, installed on different distances from the top of the satellite's shaft-holder (Deposition time 2 hrs.).

reach as high a uniformity as ± 10%, as shown in Fig. 9. In this case, the superimposed vertical scanning magnetic field was directed upwards for 55 s ($t_\uparrow$) and downwards for 45 s ($t_\downarrow$), and this sequence was repeated in the cycle during the 2-h coating deposition process. The deposition rate reached 0.8 μm/h in the uniform coating zone of 30-cm height in this process.

The coating thickness distribution over the large area, 3-D model of forming tools (dies or molds) was measured by CALOTEST on disc coupons (25-mm diam. × 4-mm thick) made of stainless steel and polished to a finish of $R_a < 100$ nm. The TiN coating was deposited for 1.5 h with single rotation without vertical scanning. Other process conditions were the same as before. Fig. 10 shows the distribution of coating thickness over this model substrate. The coating thickness (in microns) for each point is shown in brackets next to the coupon number. In this case, a deposition rate of approximately 0.8–1.2 μm/h is achieved over a 350 mm coating zone.

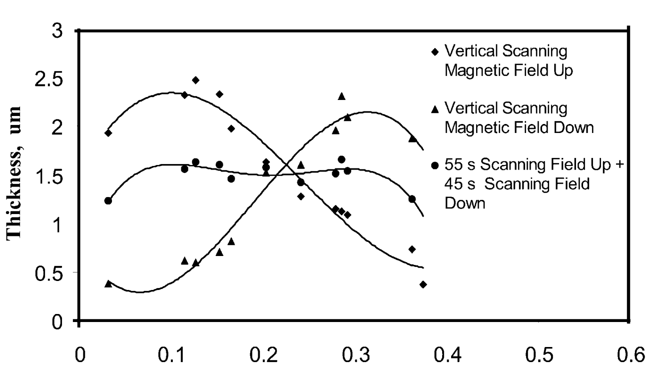

Fig. 9. TiN coating distribution of the LAFAD process with programmable vertical scanning magnetic field — deposition time, 2 h.

4. Discussion.

The density of ion saturation current coming to the substrate from the plasma can be calculated from the Bohm equation:

$$J_i \sim 0.6 n_e e (kT_e/m_i)^{0.5}$$

where n_e is electron density (equal to ion density in a quasi-neutral plasma environment), T_e is the electron temperature, k is the Boltzmann constant and m_i is the mass of ions. In the arc plasma, the value of electron density can be several orders of magnitude greater than for glow discharge, while the electron temperature is usually the same, approximately 1–3 eV [1,11,13]. Therefore, in an arc discharge it is possible to reach a much higher level of ion bombardment current on the substrate surface; approximately 0.1–10 mA/cm^2, as compared to < 0.01 mA/cm^2 for the regular RF or DC glow discharge.

A simple calculation can be used to illustrate the efficiency of the cathodic arc deposition process. The erosion rate of the metal cathodic arc targets can be determined as

$$G = \eta I_c$$

where I_c is cathodic arc current in amperes, and η(μg/C) is the characteristic erosion rate, which determines how many grams of target material will be transferred with 1 coulomb of electrical charge. Usually this value ranges between 10 and 50 μg/C for an arc current of 100 A. For a single conventional (line-of-sight deposition) cathodic arc source with a titanium target, the typical erosion rate is estimated to be in the order of $2–4 \times 10^{-5}$ g/C. For an arc source with a 100 A

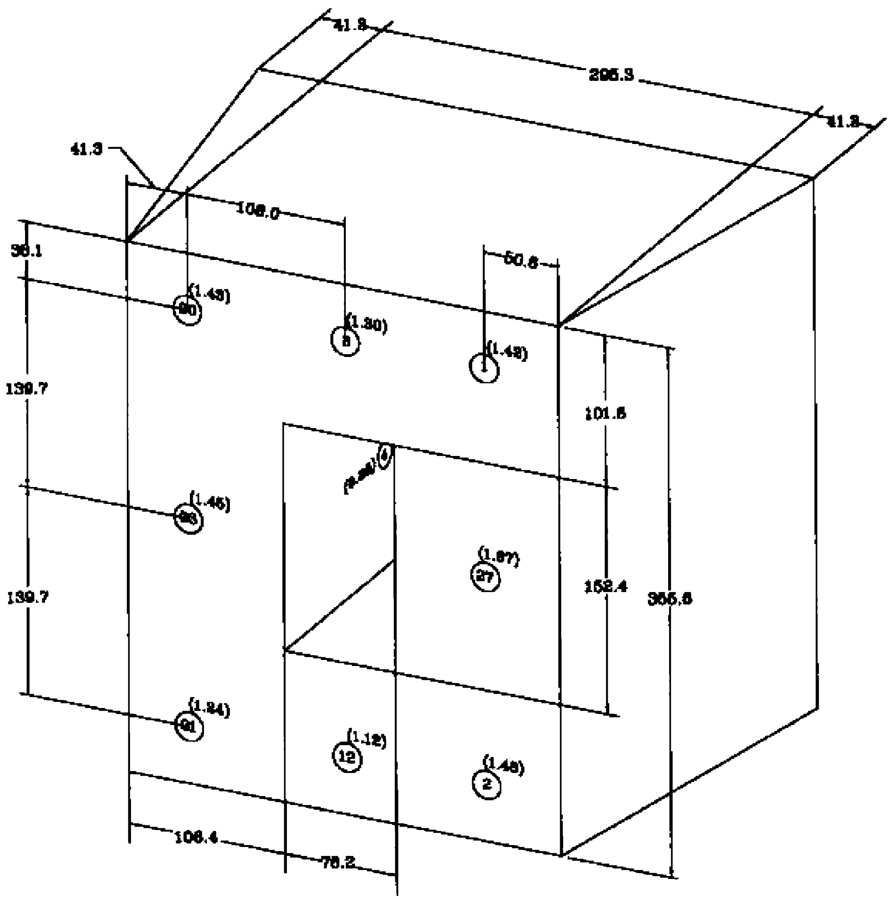

Fig. 10. TiN coating distribution of the LAFAD process over the model of a large size, complex shape forming tool — deposition time, 1.5 h.

current, this results in a flux of approximately 0.002–0.004 g/s of titanium vapor. Assuming that approximately 50% of the metal flux is lost due to macro-particles and that all the ionized species are completely transferred to the substrate, it gives a mass deposition rate of approximately 0.001–0.002 g/s. For a surface area of 1 m^2, this translates to a deposition rate of approximately 0.2–0.4 nm/s, or slightly greater than approximately 1 μm/h, which is almost the same as a dual arc LAFAS plasma source (Figs. 8–10). This fact is verified by ion current yield measurements. The ion current of 6–10 A at the exit plane of LAFAS exceeds the value obtained in a conventional vacuum -arc source with a well-focused arc plasma flow. In reality, it has been found that the large area filter design permits nearly 80% or more of the metal flux to be ionized and transferred to the substrate.

5. Conclusions

It is shown that the design of a new electromagnetic filter permits deposition of hard coatings at rates that are comparable with industrial practice, while at the same time, effectively removing the macro-particles without a significant reduction in deposition rate. The coating thickness uniformity in the vertical and horizontal (radial) directions can be substantially improved with the use of a scanning magnetic field that steers the ionized metal plasma flux uniformly to create a plasma-immersed environment in the deposition volume.

In the filtered-arc plasma-immersion technology, both the coating deposition and the treatment of substrates in the gaseous plasma environment can be achieved in a single vacuum cycle if the precursors do not interfere with each other. This includes both filtered arc, PVD coating deposition and treatment of substrates in an auxiliary-arc, gaseous plasma environment. When the deflecting magnetic coils of the LAFAS are turned off, the auxiliary arc discharge, established between the LAFAS cathodes and auxiliary anodes, provides a highly ionized gaseous plasma environment in the processing chamber. It results in high ion nitriding rate at relatively low substrate temperatures. This mode can also be used to support fast ion cleaning, ion implantation and low pressure PACVD processes at pressure ranging from 10^{-3}–1 Pa. It can also be used to enhance conventional magnetron sputtering, resistance evaporation and electron beam evaporation processes.

References

[1] D. Sanders, R. Boxman, P. Martin (Eds.), Vacuum Arc Science and Technology, Noyes Publishing, 1995.
[2] A. Aksenov, V.A. Belous, V.G. Padalka, V.M. Khoroshikh, Sov. J. Plasma Phys. 4 (1978) 425.
[3] R.L. Boxman, V. Zhitomirsky, B. Alterkop, E. Gidalevich, I. Beilis, M. Keidar, S. Goldsmith, Surf. Coat. Technol. 86–87 (1996) 243–253.
[4] A. Anders, Surf. Coat. Technol. 120–121 (1999) 319.
[5] D. Baldwin, S. Falabella, Deposition processes utilizing a new filtered cathodic-arc source, in: D. Mattox (Ed.). Proceedings of the Thirty-eighth Annual Technical Conference of the Society of Vacuum Coaters, 1995, pp. 309–316.
[6] I.I. Aksenov, V.A. Belous, V.V. Vasil'ev, Yu.Yu. Volkov, V.E. Strel'nitsij, Diam. Rel. Mater. 8 (2–5) (1999) 468–471.
[7] P.J. Martin, A. Bendavid, T.J. Kinder, L. Wielunsky, Surf. Coat. Technol. 86–87 (1996) 271.
[8] R.P. Welty, U.S. Patent No. 5-480-527, 1996.
[9] R.P. Welty, U.S. Patent No. 5-840-163, 1998.
[10] V.I. Gorokhovsky, U.S. Patent No. 5-435-900, (1995).
[11] V.I. Gorokhovsky, V.P. Polistchook, I.M. Yartsev, Surf. Coat. Technol. 61 (1993) 101–114.
[12] N. Novikov, V. Gorokhovsky, B. Uryukov, Surf. Coat. Technol. 47 (1991) 770–791.
[13] A.A. Andreev, L.P. Sablev, R.I. Stupak, V.I. Shelohaev. Proceeding of the Fourth Conference 'Vacuum Coatings-87' (in Russian), Riga, Latvia, 1987.
[14] J. Vetter, A.J. Perry, Surf. Coat. Technol. 61 (1993) 305–309.
[15] V.I. Gorokhovsky, U.S. Patent No. 5-587-207, 1996.
[16] V.I. Gorokhovsky, U.S. Patent No. 5-380-421 (1995); International Patent Application No. PCT/CA00/00380.